Oil-Assisted Agglomeration for Toner Deinking: Population Balance Model and Experiments

Bret A. Snyder and John C. Berg
Dept. of Chemical Engineering, University of Washington, Seattle, WA 98195

This study examines the selective agglomeration of hydrophobic toner particles from a repulped paper fiber slurry by adding an immiscible oil that preferentially wets the toner particles. Effects of cationic starch additives, agitation rate, time, temperature and oil composition are examined experimentally in terms of the dynamic and steady-state evolution of the particle-size distribution produced. A simple, but effective, population balance model is solved numerically to simulate the agglomeration process and provides quantitative relationships between process variables and the effectiveness and rate of agglomeration. These relations are simple and clear. The process is shown to be controlled by the composite effect of the aforementioned variables on the aggregation and breakup rates, and the observed behavior is understood in these terms. Practical recommendations for agglomeration, a process potentially useful for deinking toner-printed paper, are deduced from the results.

Introduction

Selective agglomeration of a single dispersed phase among many is a crucial step in many solid–liquid processes, such as coal beneficiation, protein precipitation, and paper deinking. Selectivity can be achieved by three general methods: manipulation of the electrostatics, such as double-layer collapse and pH control; polymer flocculation; and, less commonly, by adding an immiscible, dispersed liquid that collects solid particles of like wettability, binding them together with liquid bridges. The latter process has received sporadic attention since the early work of Farnand et al. (Farnand et al., 1961; Sutherland, 1962; Puddington and Sparks, 1975; House and Veal, 1992), and will be hereafter referred to as oil-assisted agglomeration. This article is concerned with the application of this process to deinking toner-printed papers.

Toner-printed paper, produced by laser printers and copy machines, is an increasingly abundant source of high-quality secondary fiber; however, its use is limited because effective removal of the toner is difficult (Ferguson, 1992). One promising method for toner deinking is to agglomerate the toner particles after they are released from the sheet in the repulper by adding a small amount of an appropriate insoluble liquid (Darlington, 1989; Olson et al., 1993; Snyder and Berg, 1994, 1996). The agitation in the repulper disperses the immiscible liquid into small drops that collide with the codispersed hydrophobic toner particles and hydrophilic paper fibers. The oil-like liquid drops will selectively coalesce on the hydrophobic toner surfaces, activating them for agglomeration. When the activated toner particles collide with one another, they stick through the formation of a liquid bridge. The presence of a sufficient amount of agglomerating liquid allows the process to continue until agglomerates several millimeters in diameter are formed. These can be removed from the pulp slurry later using screening or centrifugal separation.

A number of recycling mills have used agglomeration on a trial basis since its introduction at the beginning of the decade, showing both great promise and significant problems (Rhodes and Ferguson, 1993). Salient difficulties are (1) the requirement of current processes that elevated temperature, 50–60°C, be used; (2) a tendency to deposit toner mass on process equipment; and, most importantly, (3) an inconsistency in agglomeration performance, varying from excellent to useless, for incompletely understood reasons. The successful use of agglomeration demands a more fundamental understanding of the process.

In previous work, we identified five key variables in agglomeration: time, temperature, agitation rate, oil composition, and cationic starch concentration (Synder and Berg, 1994, 1996). The present work seeks to expand this by considering how the overall success of the process results from in-

Correspondence concerning this article should be addressed to J. C. Berg.

teractions of the key variables. Since an effective process requires the rapid production of an appropriate steady-state toner particle-size distribution, the problem naturally lends itself to formulation as a population balance. As the process conditions are modified, a consequent change in the competition between aggregation and breakup shifts, altering both the rate of agglomeration and its ultimate product.

Population balance modeling is a valuable method of accounting for all changes that can occur and the rate at which they do occur in the state of a population of particles (Ramkrishna, 1985). Crystallization behavior, drop-size distributions, and aerosol processes are a few applications to which population balance modeling has been applied. The core equation is developed by setting the derivative of particle size with time equal to the sum of all the aggregation and breakup rates affecting particle size.

To effectively model the process, an unambiguous set of experimental data is needed for model comparison and validation. Consequently, the objective of this study is to form a comprehensive picture of agglomeration deinking by combination of agglomeration experiments and population balance model simulations, incorporating the response of the system to the key process variables of time, temperature, agitation rate, oil composition, and cationic starch concentration.

Materials and Methods

Materials

Toner spheres were obtained from the unprinted toner powder for an Apple Laser Writer. The manufacturer (Canon U.S.A., Inc., Lake Success, NY) gives the toner composition as 55–65 wt. % styrene acryl copolymer (in approximately a 1:1 mole ratio), 30–40 wt. % magnetite (Fe_3O_4), and 1–3 wt. % salicylic acid chromium chelate. The toner comes as a powder of approximately spherical, 10–15 μm diameter primary particles, as observed in scanning electron micrographs. The toner has an advancing contact angle in water of approximately 90° and a receding angle of 70° (Snyder et al., 1993). Reserve osmosis-treated water was used for all experiments, with a conductivity equivalent to 10^{-5}-M NaCl.

Cationic starch was STA-LOK 400 (A. E. Staley Manufacturing Co., Decatur, IL), a potato starch derivatized with quaternary ammonium groups with an average of one such group for every 30 to 35 glucose units (0.30% nitrogen). These groups maintain a positive charge at all pH and salt conditions. Aqueous solutions of 1,000-ppm cationic starch were prepared by boiling 1% dry starch in water under vigorous agitation for 30 min, and diluting to obtain 1,000 ppm.

To investigate the effect of oil composition, the behavior of a pure oil was compared to that of an oil/surfactant blend. The pure oil was analytical grade *n*-hexadecane (Sigma Chemical Co., St. Louis, MO) used in previous experiments and shown to be effective when cationic starch is not present (Snyder and Berg, 1994). The oil/surfactant blend is based on a commercial formulation discovered by researchers at Betz Paperchem, Inc., and given in a series of patents (Richmann and Letscher, 1992–1994). The formulation is known to overcome the effects of cationic starch, through its solubility of starch molecules (Snyder and Berg, 1996). Furthermore, the blend is able to fuse the toners together at temperatures above 40°C, as we have observed from electron micrographs taken of toner agglomerates. The oil/surfactant blend we used is 50 vol. % *n*-hexadecane and 50 vol. % Triton X-15 (Union Carbide, Darien, CT), an octylphenol-polyethyleneoxide containing an average of 1.5 ethylene oxide units per molecule. The blend was a true solution since Triton X-15 is miscible with *n*-hexadecane. We measured an interfacial tension between the pure oil and water with the drop-weight method (Adamson, 1990), and found it to be 52 dyne/cm, while that of the oil/surfactant blend with water was 26 dyne/cm.

Methods

To perform an agglomeration experiment the following procedure was used: (1) the dispersed toner, dispersed drops, cationic starch (if used), and water were combined, adding the dispersed drops last, until a total volume of 200 mL of dispersion was created with 0.033 vol. % toner, 0.035 vol. % oil, either 0, or 1,000 ppm cationic starch. The temperature was controlled to between 23°C and 55°C by the addition of an appropriate amount of hot water. The dispersion was immediately placed in an insulated, stirred vessel and the experiment begun. (2) For all runs without cationic starch it was found that a steady-state size distribution was formed within 5 min, and so agitation was continued for 5 min; for runs with cationic starch, time studies were carried out, with runs lasting as long as 60 min. (3) At the end of an agglomeration experiment, the entire contents of the vessel were poured onto three stacked sheets of 12.5-cm Whatman-grade 41 filter paper mounted in a Büchner funnel. A vacuum pump connected to a sidearm flask provided suction. The filter paper with agglomerates was dried for study with image analysis. (4) Image analysis was performed on the agglomerates to determine the particle-size distribution. Detailed descriptions of these steps follow.

Toner was dispersed by adding 1 g of toner powder to 1 L of water and mixing in a 3.8-L Waring blender at 15,000 rpm for 2 min. The oil and oil/surfactant blend dispersions were created by adding 70 μL of the liquid to 20 mL of water and sonicating for 20 s at 40% power on a 250-W Branson probe sonicator (model 250; Branson Ultrasonics Corp., Danbury, CT). Centrifugal size analysis on a Horiba CAPA-500 (Horiba Ltd., Kyoto, Japan) showed the diameter of the drops formed to be predominantly between 0.5 and 1.5 μm. The ratio of the volume of oil to the volume of toner is an important variable for oil-assisted agglomeration, and our previous work showed that the most effective ratio for toner powder is 1:1 (Synder and Berg, 1994). Therefore, this was used in all experiments.

Temperature was maintained by keeping the dispersion well-insulated during a run. One and a half centimeters thick foam insulation encased the agglomeration vessel. Temperatures reported are starting temperatures; temperature gradually fell in the vessel in an exponential manner, in accord with Newton's law of cooling, with a characteristic decay time of 107 min.

The vessel used for agglomeration was a Virtis "23" Homogenizer (Virtis Corp., Gardiner, NY) of spherical-type shape, 7 cm high and 9 cm in diameter. It had five baffles built into the walls, evenly spaced and protruding 0.5 cm. The vessel was made of glass that was hydrophobized by Scotch-

guard (3M, St. Paul, MN) fluorocarbon coating to reduce adhesion of oil and toner to its surface. Agitation was provided by a vertical shaft. There were four stainless-steel blades, one opposite pair on the end of the shaft and the other oppositely mounted pair 1 cm above the end. Looking axially along the shaft, the blades were set apart 90°. Each blade was 2 cm long and 1 cm wide, rectangular with rounded corners, and angled 30° from horizontal. Impeller motion directed liquid flow downwards along the shaft.

We found that the useful range of rotational rates was from 900 to 2,900 rpm. Below 900 rpm, insufficient churning of the bulk liquid occurred for it to mix well and allow agglomeration. Although speeds up to 23,000 rpm were available, our experiments showed no advantage in increasing shear above 2,900 rpm, as described in the results and discussion section on the effect of shear rate. To determine the shear rate corresponding to a given rpm, a thermocouple was inserted into liquid and the temperature monitored under agitation. The rise in temperature with time indicated the mechanical energy dissipated in the water; ϵ, the energy dissipated per unit mass, is then calculated by dividing the energy consumption by the mass of water. The square root of the ratio of ϵ to the kinematic viscosity of water provides G, a measure of the average rate of shear.

Image analysis was done with a Wild M420 Makroskop (Wild Heerbrugg Ltd., Heerbrugg, Switzerland) macroscope attached to an MTI 65 video camera (DAGE-MTI, Inc., Michigan City, IN). Output from the camera went into a Data Translation (Data Translation, Inc., Marlboro, MA) frame-grabber board. NIH Image freeware, version 1.60b7 (National Institute of Health, Bethesda, MD), was used to analyze the images and obtain particle size counts. To collect the image data, 100× total magnification was used, providing a 0.8-by-1.0-cm image area. The advantage of high magnification is the ability to observe the smallest particles; the disadvantage is the small sample area on the filter paper. At the used magnification, the smallest measurable particle size is 21 μm. We took numerous samples of the filter paper at randomly selected locations. A minimum of 500 particles was counted for a sample; typically 1,000 were observed. For samples with a very high degree of agglomeration, we imaged all the particles that were found on the sheet. The data that resulted consisted of a list of particle areas observed by image analysis, and this was fed into KaleidaGraph (Synergy Software, Warrington, PA, Version 3.0) and from each particle area an equivalent "circular" particle diameter was extracted by calculating the diameter of a circle of equivalent area: diameter $= (4 * \text{area}/\pi)$.

For determining statistics on the particle-size distributions, the characteristic size was calculated as the diameter of a particle of average volume. This is the diameter of the particle of average mass and provides a good measure of where the bulk of the toner resides in the size spectrum. Thus, the average volume, $\bar{v}$, is calculated as

$$\bar{v} = \frac{\sum_i n_i v_i}{\sum_i n_i}, \tag{1}$$

and the corresponding average particle diameter, $\bar{d}$, is then given by

$$\bar{d} = \left(\frac{6}{\pi}\bar{v}\right)^{1/3} \tag{2}$$

Standard deviation and skewness were calculated similarly.

Each experimental point was the average of from two to six experiments. Variations between identical runs were rather large; thus the need for averaging. Relative error of the average particle diameter was typically 12%.

Model Description

The population balance model was developed by writing equations to account for the growth and breakup of aggregates. We started from the method described by Hounslow et al. (1988) and then rewrote the equations using volume fraction as the independent variable instead of number density, as Hounslow et al. used. We first used number density in our simulations, but model convergence was too slow and showed great improvement with volume fraction as the independent variable. No difference in results between the methods was found. The essence of the method is to discretize the spectrum of particle sizes into n bins such that the size bins are spaced geometrically, and then simultaneously solve the n differential equations. The physics of the process, of course, remains in the rate expressions used for aggregation and breakup.

The basic equation can be expressed in words as follows: (change in time of aggregates at size i) = (rate of gain in size i by aggregation of particles smaller than size i) + (rate of gain in size i by breakup fragments produced by the breakup of particles larger than size i) − (rate of loss in size i by aggregation of particles in size i to form aggregates larger than size i) − (rate of loss in size i by breakup of particles in size i to fragments smaller than size i).

The aggregation-rate expression is drawn from the literature, following the expression of Camp and Stein (1943), which is cast in number density. Adding the aggregation efficiency, α, which represents the number of collisions that result in aggregation over the number of theoretically occurring collisions (Ayazi Shamlou and Titchener-Hooker, 1993), and converting to volume fraction as the independent variable, we obtain the following expression for the increase in volume fraction in the $i+j$ bin from aggregation events between particles in the i and j bins:

$$\frac{dx_{i+j}}{dt} = \frac{4}{3}\alpha V\left(\frac{\epsilon}{\nu}\right)^{1/2}\left(\frac{1}{v_i}+\frac{1}{v_j}\right)\left(v_i^{1/3}+v_j^{1/3}\right)^3 x_i x_j. \tag{3}$$

The breakup rate expression has to account for the inherently complex breakup process. Unlike aggregation, several mechanisms of breakup can occur in the same system (Ayazi Shamlou and Titchener-Hooker, 1993). We followed other investigators, such as Grabenbauer and Glatz (1981) and Chen (1992), and used a single power-law relation to express the increasing tendency of the particles to break up as they get larger. We experimented with other forms for the breakup rate dependence on particle size, particularly with an exponential dependence, but the results did not fit the experimental data. The expression we used is

$$\frac{dx_i}{dt} = -B\left(\frac{d_i}{d_1} - 1\right)^{\nu} x_i. \tag{4}$$

This shows the rate of loss of particles in bin i by breakup. B is the (dimensional) breakup rate constant, while $[(d_i/d_1)-1]^{\nu}$ accounts for the dependence of the breakup rate on the size of the breaking particle. The expression is written so that the breakup rate is by definition zero for particles in the smallest size bin. The exponent, ν, is left as a parameter in the model.

To specify the breakup rate completely, we must also describe the size of the breakup fragments formed. As well known in the literature, particle breakup can occur by splitting and erosion, which represent the extremes of a continuum (Ayazi Shamlou and Titchener-Hooker, 1993). In splitting, particles form a few large fragments; in erosion, ablation removes small particles from a large particle's surface. We decided to use the simplest possible expression that allows either of these mechanisms to occur. We allowed a particle to break up only into two daughter particles. Then we accommodated both splitting and erosion by including a parameter, p, that is the ratio of the mass of the smaller breakup particle to the particle mass. Therefore, if $p = 0.5$, particles only split into equal halves; if $p = 0.01$, particles split into one with 99% of the mass and the other with 1% of the mass. We obtained close fits to experimental data with this expression.

These equations are nondimensionalized by using the variables, τ, β, and ρ, which are the nondimensional time, breakup rate, and ratio of breakup rate to aggregation rate, respectively. These are given by

$$\tau = \alpha V G t, \tag{5}$$

$$\beta = \frac{B}{G}, \tag{6}$$

$$\rho = \frac{B}{\alpha V}, \tag{7}$$

yielding for the aggregation and breakup expressions:

$$\frac{dx_{i+j}}{d\tau} = \frac{4}{3}\left(\frac{1}{v_i} + \frac{1}{v_j}\right)\left(v_i^{1/3} + v_j^{1/3}\right)^3 x_i x_j \tag{8}$$

$$\frac{dx_i}{d\tau} = -\rho\left(\frac{d_i}{d_1} - 1\right)^{\nu} x_i. \tag{9}$$

The model simulation used 30 bins, each bin twice the size of the previous one. We thereby covered a 10^3 range in particle diameter, from 10 μm to 10,000 μm. The resulting system of nonlinear differential equations is of the form

$$\frac{dx_i}{d\tau} = \sum_{j=1}^{n}\sum_{k=1}^{n} A_{ijk} x_j x_k + \sum_{j=1}^{n} B_{ij} x_j, \tag{10a}$$

with initial condition

$$x_i(0) = x_{0,i} \tag{10b}$$

for dynamic simulations. This simplifies for the steady-state case to

$$0 = \sum_{j=1}^{n}\sum_{k=1}^{n} A_{ijk} x_j x_k + \sum_{j=1}^{n} B_{ij} x_j. \tag{11}$$

The key information comes in the coefficients A_{ijk}, a third-order tensor that contains the aggregation information, and B_{ij}, a second-order tensor that contains the breakup information. Both of these are formed at the beginning of the simulation, as they depend only on model parameters and then remain fixed during the course of the problem solution.

The population balance model was solved by a program written for Matlab 4.2.1 (The MathWorks, Natick, MA). Numerical solution was obtained using a 4th-to-5th-order Runge-Kutta method or a nonlinear equation solver. Simulation times for steady-state problems were usually about 30 s on a PowerMac 7100/66; the dynamic solutions took longer, especially as steady state was approached, running as long as 30 min. The input consisted of values for the parameters α, β, and V, which are used to calculate ρ, ν, and p. The latter three are the only independent parameters in the model. Using these as input, the evolution of the particle-size distribution in time (Eqs. 10a, 10b) or just the steady-state particle-size distributions (Eq. 11) is produced, depending on the mode in which the model is operated, to produce a smooth size distribution. Statistics were calculated from the simulation results in the same manner as they were from the experimental data.

Results and Discussion

Experiments

The experiments clearly showed a strong effect of agitation rate on the particle size obtained. Figure 1 shows a plot of average particle diameter vs. shear rate, comparing the behavior of the pure oil and the oil/surfactant blend. Agglomerate size in both cases falls with increasing shear rate in an approximately linear fashion over the range of shear rates examined. Increasing shear rate increases both the frequency of collision and the likelihood of particle breakup. However, as Figure 1 shows, the tendency to break up predominates. Equally important, we see that at all shear rates, the pure oil produces larger agglomerates than the oil/surfactant blend. Since these data are collected at a low temperature where no fusion of the toner particles occurs (Snyder and Berg, 1996), liquid bridges alone hold the aggregates together. The strength of these is directly proportional to the interfacial tension (Newitt and Conway-Jones, 1958; Pietsch, 1990). Therefore, we expect the agglomerating liquid with the higher interfacial tension to produce stronger agglomerates, and indeed this is what we observe. In fact, we find a direct proportionality between the interfacial tension and size of the agglomerates; the pure oil has both twice the interfacial tension and twice the average particle diameter. This is expected from previous work (Newitt and Conway-Jones, 1958; Pietsch, 1990). The results indicate the importance of agglomerate strength for successful agglomeration.

It should be noted that the results presented in Figure 1 represent the trends only over the shear range accessible with

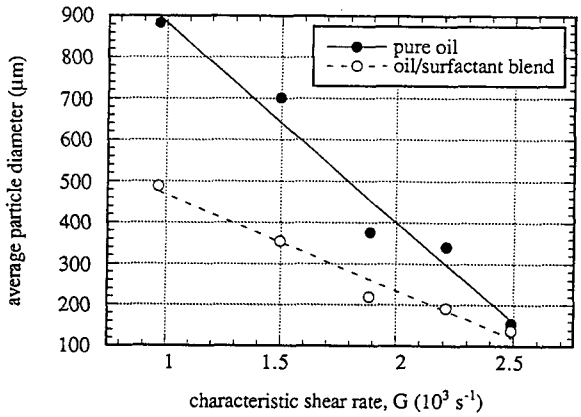

Figure 1. Average particle diameter vs. shear rate in the aggregation vessel.

G = 1,000 s^{-1} corresponds to 900 rpm; G = 2,500 s^{-1} corresponds to 2,900 rpm.

our experiment; lower shear rates did not provide adequate mixing, while higher rates were not tested, as these were considered unrealistic for typical agglomeration and, in addition, it is clear that little additional size reduction could be expected in any case since the aggregates are already made quite small at the highest shear rate used. Certainly, if the graph were extended into very low shear, we would see a reduction in aggregate size as we enter a region where mixing was insufficient to bring the particles together.

Figure 2 shows the effect of temperature on pure oil and the oil/surfactant blend compared. Dramatically different behavior is observed. While the pure oil produces agglomerates of a fixed size at all temperatures, we see a large increase in particle size produced with the oil/surfactant blend as the temperature is raised. We previously examined the agglomerates formed at a high temperature for both types of oil with electron microscopy and found the oil/surfactant blend to fuse the primary toner particles into a much larger, cohesive toner sphere, thereby significantly augmenting the aggregate strength. This increase in aggregate strength fosters the formation of larger particles, emphasizing its importance.

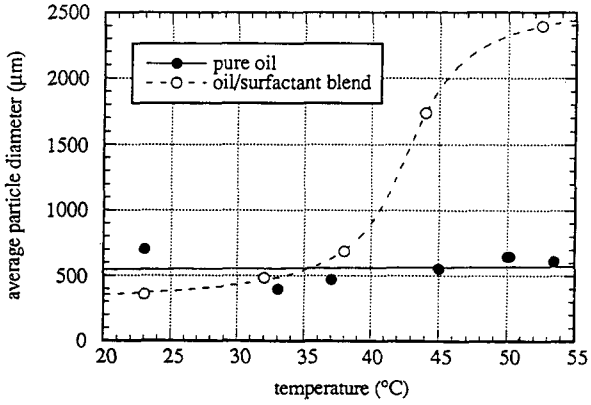

Figure 2. Average particle diameter vs. temperature.

While temperature has no effect on the size of agglomerates produced from pure oil, high temperature drastically increases the size of oil/surfactant agglomerates by fusing them together into aggregates of high strength.

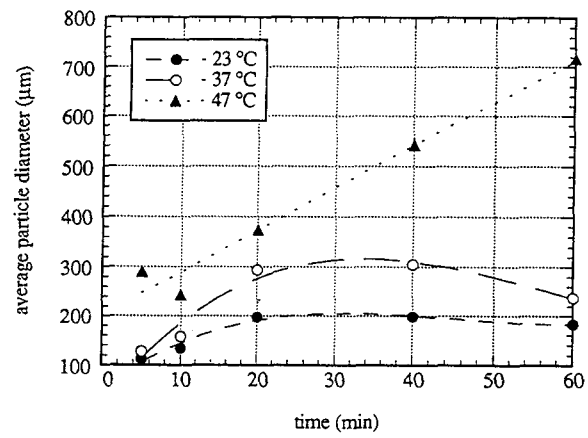

Figure 3. Average particle diameter vs. time; oil/surfactant blend with 1,000 ppm cationic starch at 23, 37, and 47°C.

Increasing temperature increases particle size by strengthening the agglomerates, but the entire aggregation process still requires 30 min or more to reach full-size, steady-state agglomeration.

Figure 3 depicts the results when cationic starch is present. We have done extensive work on the effect of cationic starch on agglomeration, first identifying it as a key agent for controlling the course of agglomeration (Snyder and Berg, 1994), and then examining how it affects agglomeration (Snyder and Berg, 1996). Cationic starch, or other cationic polyelectrolyte, is generally present in paper furnishes as a retention aid to bind filler particles into the paper web or to size the paper, and a significant amount redissolves in the repulper (Marton and Marton, 1976). The conclusion of the latter investigation clearly indicated that cationic starch adsorbs to toner, pure oil, and oil/surfactant interfaces, providing a barrier to coalescence of the interfaces. However, the oil/surfactant interface possesses the important property of engulfing the cationic starch adlayer, and thereby removing its steric barrier to coalescence and providing the possibility of engulfing the adlayer on the toner as well. This has been proven by a combination of adsorption, electrokinetic, wettability, and adlayer thickness measurements (Snyder and Berg, 1994, 1996). Since the pure oil has no ability for adlayer engulfment, agglomeration is effectively prevented by high concentrations of cationic starch, such as the 1,000 ppm used here.

Figure 3 shows agglomeration in the presence of cationic starch when the oil/surfactant blend is used. First of all, we notice that the time needed to reach the maximum particle size is at least 30 min, much longer than the 3 min observed when cationic starch is not present. The explanation is that cationic starch reduces the agglomeration rate by reducing the rate at which droplets and toner particles coalescence. The number of collisions per time is the same, but the efficiency of collisions, α, is reduced, because of the stabilizing effect of the cationic starch adsorption (Snyder and Berg, 1996). This reduction not only slows agglomerate growth, it also reduces the steady-state particle-size distribution because this exists where the aggregation and breakup rates balance, and therefore lowering the aggregation rate shrinks the steady-state size distribution.

The effect of temperature in Figure 3 is similar to that in

Table 1. Average Relative Deviation and Skewness for Experimental Distributions*

	Rel. Dev., $s/\bar{d}$	Skewness, κ
0-ppm cationic starch	1.72 ± 0.08	9.36 ± 1.39
1,000-ppm cationic starch	2.00 ± 0.09	17.62 ± 1.64
All experimental runs	1.83 ± 0.06	12.80 ± 1.06

*A significant increase in both occurs when cationic starch is present. The variations reported are the standard errors.

Figure 2: increasing temperature with the oil/surfactant blend produces stronger agglomerates, and thereby increases the ultimate particle-size distribution. Clearly, in Figure 3, the sizes obtained are much smaller than in Figure 2 at the same temperature, showing the potent effect of cationic starch, even though the oil/surfactant blend possesses some ability to operate in its presence. In a practical sense, Figure 3 indicates the importance of using long run times when agglomerating with high levels of cationic starch.

To facilitate meaningful comparison of the model and the experimental results, the full experimental size distributions were examined. The distributions making up the individual data points in Figures 1–3 had significant variation and were not well-suited to a least-squares fitting of each size distribution by the model. Instead, three statistics of the experimental data were used: the average particle diameter, $\bar{d}$, the relative deviation of particle sizes, $s/\bar{d}$, and the skewness, κ. The variations of $\bar{d}$ with experimental conditions were of course significant; however, $s/\bar{d}$ and κ generally exhibited no trends with experimental conditions. Therefore, the average values of $s/\bar{d}$ and κ, and knowledge of $\bar{d}$, were found to contain the information needed for predicting a particular size distribution. The only exception to this is the significant difference in both $s/\bar{d}$ and κ between runs with and without cationic starch. Table 1 presents the characteristic relative deviation and skewness for both the cationic starch and non-cationic starch experiments. The presence of cationic starch increases the relative deviation by 16% and the skewness by 88%. Thus, it causes the formation of broader distributions, with a tendency for several large particles to be present amidst a great number of small particles. We believe this results from cationic starch acting unevenly on toner particles, completely preventing some from coalescence and less drastically retarding the coalescence of others. Such behavior could result from uneven adsorption of cationic starch; for instance, some toners may have different surface chemistry, depending on the material exposed predominantly on its surface, with some materials more favorable to cationic starch adsorption and hence more conducive to the development of electrosteric stabilization.

Population balance model

In dimensionless form, the model has three independent parameters: the relative rate constant of breakup to aggregation, ρ, the breakup rate exponent of particle volume, ν, and the volume fraction of a breakup daughter particle to the parent, p. The effect of the first is to control the average particle size produced; the second determines the spread in the particle-size distribution; and the third most influences the shape, and hence, the skewness of the distribution. Figure 4 presents a fit of one experimental size distribution by the model. The experimental size distribution is relatively smooth, and thus we expect a close fit by the model, and indeed this is what is found. The fits obtained by matching $\bar{d}$, $s/\bar{d}$, and κ as closely as possible produced very satisfactory results, such as those shown in Figure 4.

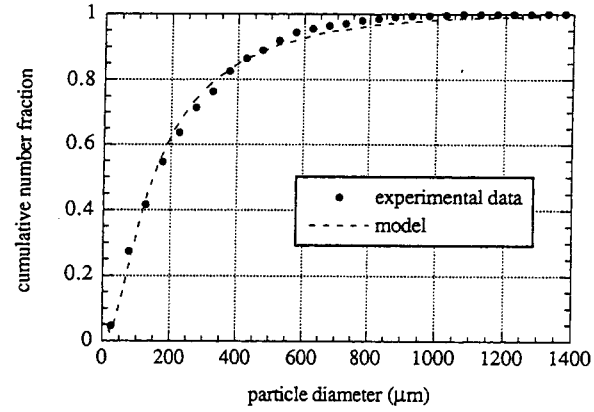

Figure 4. Comparison of the experimental data to the best fit of the population-balance model.

Figure 5 shows the time-evolution of size distributions predicted by the model for sample conditions. Clearly, a smooth increase in particle size occurs until steady state is reached. A plot of average particle size vs. time shows that the growth exhibits a slightly sigmoidal behavior.

In order for the population-balance model to correctly fit the experimental data, the three parameters, ρ, ν, and p, must be properly chosen. The best fits are obtained when $p = 0.5$, indicating that particle breakup occurs predominantly by a splitting mechanism, and therefore not by erosion. Furthermore, ν is found to be either 0.735 when 1,000 ppm cationic starch is present or 0.884 when it is not present, indicating that the particle breakup rate is proportional to the particle diameter to a power somewhat less than 1; 0.735 for 1,000 ppm cationic starch, 0.884 for 0 ppm cationic starch. All changes in particle size are accounted for by changes in ρ, the ratio of aggregation rate to breakup rate constants. Thus, as experimental conditions vary, it is ρ that varies,

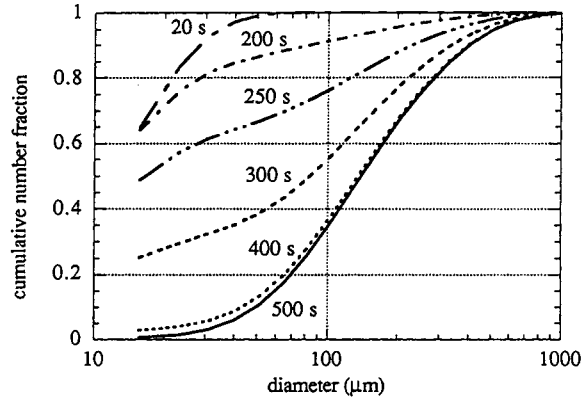

Figure 5. Evolution of particle-size distributions in time predicted by the population-balance model for typical conditions.

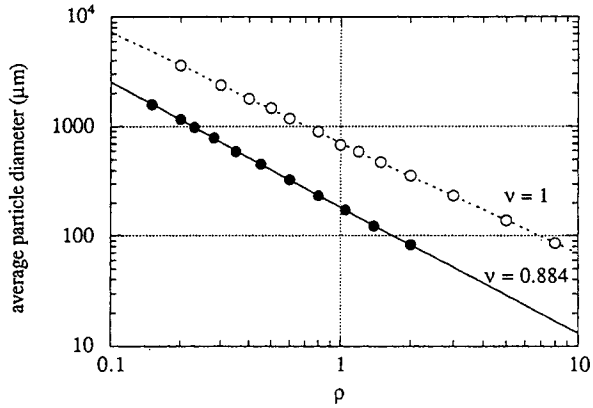

Figure 6. Population-balance model: average particle diameter vs. relative rate constants of aggregation and breakup, ρ, holding ν, and p constant.

Two values of ν are compared, $\nu = 0.884$ and $\nu = 1$. The fit lines are $\bar{d} = k\rho^{-1/\nu}$, where k is a constant.

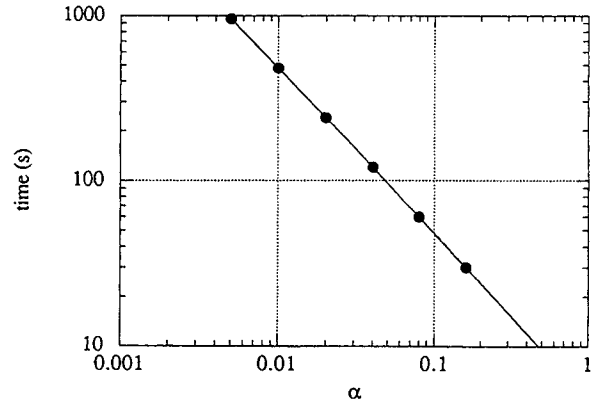

Figure 7. Time to reach steady-state average particle diameter vs. aggregation, α.

The fit line is time = $4.8/\alpha$. Thus, the time to reach full aggregation is inversely proportional to the aggregation efficiency. Typical conditions for other parameters were used: $\nu = 0.884$; $p = 0.5$; $G = 1{,}500\ s^{-1}$; $\rho = 0.4$.

changing the particle size, while ν and p remain essentially constant.

When only ρ varies, it is readily related to the average particle diameter:

$$\bar{d} = k\rho^{-1/\nu}, \tag{12}$$

where k is a constant with units of length. For $\nu = 0.884$ (no cationic starch present), $k = 1.86 \times 10^{-4}$ m. When $\nu = 1$, the simple inverse relationship obtains; in our systems, however ν is slightly less than 1, so the average diameter falls more steeply with ρ. Figure 6 shows the effect of varying ρ on $\bar{d}$.

Table 2 presents the relationships between the model parameters and the size distribution statistics. It is observed that ρ controls the particle size, ν controls the spread of particle sizes at steady state, and p controls the skewness of the distribution, but not in a simple manner. Intuitive physical reasoning supports all these relationships: the balance of aggregation and breakup rates determines the ultimate particle size, the sensitivity of the breakup rate on particle size determines the compactness of the distribution about its average, and reducing the size of the daughter particle formed on breakup increases the number of smaller particles while leaving a few large ones.

While ρ, the ratio of the breakup and aggregation rates, determines the steady state particle size, the absolute value of αVG determines the time needed to reach steady state. Since V and G are fixed in an experiment, it is α that effectively fixes the time for full agglomeration. This is shown in Figure 7. When experimental determination of the time needed to reach steady state is available, α can be numerically evaluated when V and G are known. Analyzing our experimental data, we find for the case when cationic starch is not present, $\alpha \approx 0.04$, since steady state is found to be achieved in about 3 min. In 1,000-ppm cationic starch, $\alpha \approx 0.004$ or less, corresponding to 30 min or more needed to reach the steady state, as shown in Figure 3. Thus, 1,000 ppm cationic starch reduces the collision efficiency of aggregation by at least an order of magnitude, even in the presence of the oil/surfactant blend.

Table 2. Principal Relationships Between Model Parameters and Size-Distribution Statistics*

Model Parameter	Size-Distribution Statistic	Relationship
ρ	$\bar{d}$	$\bar{d} = k\rho^{-1/\nu}$
ν	$s/\bar{d}$	$s/\bar{d} = k\nu^{-2/3}$
p	κ	Complex; as $p \downarrow$, $\kappa \uparrow$

*The relationship obtains when the other two model parameters are held constant.

By combining the model results with the observed experimental trends, quantitative relations can be found between agglomeration response and operating variables. For instance, using the linear trends of particle size with shear in Figure 1, the general equation is

$$\bar{d} = k_1\sigma(k_2 - G). \tag{13}$$

The best fit values give $k_1 = 9.13 \times 10^{-6}\ m^2 \cdot s^3 \cdot kg^{-1}$ and $k_2 = 2{,}910\ s^{-1}$. Equation 13 shows that the average particle diameter is directly proportional to the oil–water interfacial tension, σ. Since both the crushing strength and the tensile strength for liquid bridge agglomerates are also found to be linearly proportional to σ (Newitt and Conway-Jones, 1958; Pietsch, 1990), we conclude that the average agglomerate diameter is directly proportional to particle strength, as given by σ. To develop a relation between B, the absolute breakup rate constant, and the particle strength, σ, we combine Eqs. 6, 7, 12 and 13 to find

$$B = k_3 \frac{1}{\sigma^{\nu}}. \tag{14}$$

Since ν and p are found to be constant for the agglomeration systems studied here, the population-balance model indicates that changes in ρ are the only way to influence the steady-state particle-size distribution. Furthermore, we have

seen that the aggregation rate alone controls the rate at which agglomeration proceeds to its steady-state configuration. Therefore, all of our experimental variables can be shown to affect either the aggregation rate, α (cationic starch), or the breakup rate, β (oil composition, temperature, agitation rate). Time does not affect either of these directly, of course, but the time needed for full agglomeration depends on α.

Conclusions

We have demonstrated how and why process conditions and ingredients control the success of oil-assisted agglomeration, using the collection of dispersed toner particles as our model system. By combining experimental investigations with a population-balance model, a series of simple equations were found to express the dependence of the particle-size distribution on time, temperature, agitation rate, oil composition, and cationic starch presence. The experimental data followed a universal curve where a single parameter, here taken as the average particle size, predicts the particle-size distribution.

The population balance model is simple but still captures the important physics of the process. It contains only three parameters, but produced agreement with experimental-size distributions. The ratio of breakup to aggregation contains the essential information on which successful agglomeration depends. Cationic starch affects this by reducing the aggregation rate through lowering the collision efficiency, and so both slowing the rate of agglomeration and its ultimate size. The factors temperature, agitation rate, and oil composition interact by controlling the breakup rate, and through this, influencing the agglomerate size-distribution. The simple relation between particle size and aggregation and breakup rates was quantitatively expressed.

In a practical sense, this study stresses the need to reduce agitation rate as much as feasible during agglomeration, the need to allow long times when high levels of cationic starch are present, and the need to develop oil formulations that yield the strongest agglomerates. From a phenomenological consideration, we have demonstrated how oil-assisted agglomeration operates and how it can be effectively modeled, observing relatively simple relations between the important quantities to provide a clear conception of the underlying physics of the process.

Acknowledgments

The authors gratefully acknowledge the financial support of the Weyerhauser Foundation, Fisken Fellowship Program

Notation

i, j, k = indices for bins
k, k_1, k_2, etc. = constants obtained from data fitting; dimensions as given in the text
s = the standard deviation of a particle-size distribution, μm
t = time, s
v_i = characteristic particle volume for bin i
V = volume fraction of aggregating particles in fluid
x_i = volume fraction of all dispersed particles in bin i
ν = exponent expressing dependence of breakup rate on particle diameter; also kinematic viscosity of fluid, m^2/s

Literature Cited

Adamson, A. W., *Physical Chemistry of Surfaces*, 5th ed., Wiley, New York, p. 21 (1990).

Ayazi Shamlou, P., and N. Titchener-Hooker, "Turbulent Aggregation and Breakup of Particles in Stirred Vessels," *Processing of Solid-Liquid Suspensions*, P. Ayazi Shamlou, ed., Butterworth-Heinemann, Oxford, p. 1 (1993).

Camp, T. R., and P. C. Stein, *J. Boston Soc. Civ. Eng.*, **30**, 219 (1943).

Chen, W., "Protein Precipitation by Polyelectrolytes," PhD Diss., Dept. of Chemical Engineering, Univ. of Washington, Seattle (1992).

Darlington, W. B., "A New Process for Deinking Electrostatically-Printed Secondary Fiber," *Tappi J.*, **72**, 35 (1989).

Farnand, J. R., H. M. Smith, and I. E. Puddington, "Spherical Agglomeration of Solids in Liquid Suspension," *Can. J. Chem. Eng.*, **39**, 94 (1961).

Ferguson, L. D., "Deinking Chemistry: 1," *Tappi J.*, **75**, 75 (1992).

Grabenbauer, G. C., and C. E. Glatz, "Protein Precipitation—Analysis of Particle Size Distribution and Kinetics," *Chem. Eng. Commun.*, **12**, 203 (1981).

Hounslow, M. J., R. L. Ryall, and V. R. Marshall, "A Discretized Population Balance for Nucleation, Growth, and Aggregation," *AIChE J.*, **34**, 1821 (1988).

House, C. I., and C. J. Veal, "Spherical Agglomeration in Mineral Processing," *Colloid and Surface Engineering: Applications in the Process Industries*, R. A. Williams, ed., Butterworth-Heinemann, Oxford (1992).

Marton, J., and T. Marton, "Wet-End Starch: Adsorption of Starch on Cellulosic Fibers," *Tappi J.*, **59**, 121 (1976).

Olson, C. R., J. D. Hall, and I. J. Philippe, "Laser Print Deinking Using Chemically-Enhanced Densification and Forward Cleaning," *Prog. Paper Recycling*, **3**(2), 24 (1993).

Newitt, D. M., and J. M. Conway-Jones, "A Contribution to the Theory and Practice of Granulation," *Trans. Instn. Chem. Engrs.*, **36**, 422 (1958).

Pietsch, W., *Size Enlargement by Agglomeration*, Wiley Interscience, Chichester, England (1990).

Puddington, I. E., and B. D. Sparks, "Spherical Agglomeration Processes," *Minerals Sci. Eng.*, **7**, 282 (1975).

Ramkrishna, D., "The Status of Population Balances," *Rev. Chem. Eng.*, **3**, 49 (1985).

Rhodes, T., and L. D. Ferguson, "Deinking Non-impact Printed Office Waste: A Mill's Perspective," *TAPPI 1993 Recycling Symposium*, Tappi Press, Atlanta, GA, p. 213 (1993).

Richmann, S. K., and M. B. Letscher, "Process and Composition for Deinking Dry Toner Electrostatic Printed Wastepaper," U.S. Patent No. 5,141,598 (1992); "Use of Surfactants Having an HLB Less than 10 in the Deinking of Dry Toner Electrostatic Printed Wastepaper," U.S. Patent No. 5,200,034 (1993) and U.S. Patent No. 5,248,388 (1993); "Process and Composition for Deinking Dry Toner Electrostatic Printed Wastepaper," U.S. Patent No. 5,302,242 (1994). (All assigned to Betz Paperchem, Inc., Jacksonville, FL.)

Snyder, B. A., and J. C. Berg, "Deinking Toner-Printed Paper by Selective Agglomeration," *Pulp Paper Can.*, **97**, 38 (1996).

Snyder, B. A., and J. C. Berg, "Liquid Bridge Agglomeration: A Fundamental Approach to Toner Deinking," *Tappi J.*, **77**, 79 (1994).

Snyder, B. A., D. C. Schmidt, and J. C. Berg, "Characterization and Flotation Studies of Electrostatic Inks," *Prog. Paper Recycling*, **3**(1), 17 (1993).

Sutherland, J. P., "Agglomeration of Aqueous Suspensions of Graphite," *Can. J. Chem. Eng.*, **40**, 268 (1962).

Manuscript received Sept. 27, 1996, and revision received Jan. 3, 1997.